Hygrothermal Effects on Structure-Borne Noise Transmission of Stiffened Laminated Composite Plates

Constantinos S. Lyrintzis*
San Diego State University, San Diego, California
and
Dimitri A. Bofilios†
Integrated Aerospace Sciences Corporation, San Diego, California

This paper examines the effect of elevated temperatures, absorbed moisture, and random external excitation on the dynamic response and structure-borne noise transmission of discretely stiffened flat plates from laminated composite material. An analytical approach using modified transfer matrices for composite stiffened flat panels, including the hygrothermal effects, is developed to obtain the required dynamic response solution. Ingestion of moisture and changes of temperature levels were taken to vary linearly with the swelling, which results in effective force resultants. The dynamic response is calculated from the total hygrothermal and mechanical loading environment. The theoretical solutions of the governing acoustic-structural equations for the transmitted noise are obtained using modal decomposition. The acoustic enclosure is taken to be rectangular in shape, a portion of its boundaries is elastic (composite material), while the remaining surface is acoustically rigid. Numerical results are presented for acousto-structural applications revealing the hygrothermal effect on composite materials.

Introduction

THE surface protection systems of aerospace and aircraft structures are constructed more often lately from discretely stiffened composite components. The vibrations induced from various sources could generate structure-borne noise in the interior of aircraft and space transportation vehicles. Problems arise due to a significant degree of unpredictability of loads, thermal and hygrothermal effects, and materials behavior under adverse conditions. The vibroacoustic environment of the aerospace structures is directly affected from any uncertainty in the response and transmitted sound predictions. This presents a challenge to develop a new technology based on analytical and experimental methods for noise and vibration control.[1]

Interior noise in most transportation vehicles is dominated by low-intermediate frequency noise. A considerable effort has been made recently toward understanding and solving noise transmission problems. Numerical solutions using finite-element methods are used extensively, but are limited to the low-frequency range, and require large computer storage capabilities. Statistical energy analysis has been used, but the method loses its effectiveness when structural and/or acoustic modes are well separated and its inputs are dominated by discrete peaks. Analytical studies of noise transmission start from the representation of the structural model. Analytical models can predict the sound transmission levels at the intermediate-frequency range. An analytical approach for structure-borne noise generation was developed in Refs. 2 and 3 for a composite shell with point loads. These models did not account for the discrete stiffening effect. Procedures have been developed in Refs. 4–9 to study response and noise transmission of stiffened and interconnected structures constructed from homogeneous and isotropic materials and a rectangular acoustic enclosure. Lately, structural models were presented for stiffened structures from composite materials.[10] However, all of those approaches pertain only to elastic bodies at one temperature, which is the stress free temperature if it is under no loads. Changes in temperatures are commonplace in composite materials, both during fabrication and during structural usage.[11,12] There are two important effects of the temperature. First, most materials expand when heated and contract when cooled, and second, the stiffness changes (most materials become softer, more ductile and weaker as they are heated).[13,14] It was also shown that significant changes in the mechanical properties of fiber-reinforced polymeric composite may result from the combined effects of absorbed moisture and thermal environment.[11,15–17] Thus, it is imperative to assess the extent of their effects upon performance. It was realized that the ingestion of moisture varied linearly with the swelling, so that an effect similar to the thermal effect is observed.[15,16]

This paper presents an analytical study to predict dynamic response and noise transmission of discretely stiffened multilayered composite panels and examines the effects of the temperature and high humidity. A typical geometry of a stiffened panel is shown in Fig. 1 and a rectangular enclosure in Fig. 2. A transfer matrix procedure has been developed to model the composite stiffened panels.[10] The present approach extends the procedures to include the hygrothermal effects on the stiffeners and on the panels. The transfer matrices were modified to include the coefficients of thermal and hygrothermal expansion. The sound pressure levels in the interior are obtained by coupling the acoustic field to the sidewall vibrations of the stiffened structure.[5,9,10] Modal decomposition of the interior acoustic pressure is used together with the point impedance representation of the interior acoustic absorption characteristics.

Temperature and Moisture Concentration Functions

Consider a laminate composed of N laminae. All laminae are anisotropic containing a single plane of elastic symmetry and subjected to environmentally induced deformations resulting from changes in temperature and absorption or desorption of moisture. Thermoelastic deformations are assumed to be accurately described by linear coefficients of thermal expansion over the range of temperatures of interest.[12] Similarly, the deformations induced by the hygroscopic nature of the lamina

Received Sept. 9, 1989.

*Assistant Professor, Department of Aerospace Engineering and Engineering Mechanics. Member AIAA.
†Technical Director, Department of Research and Development. Member AIAA.

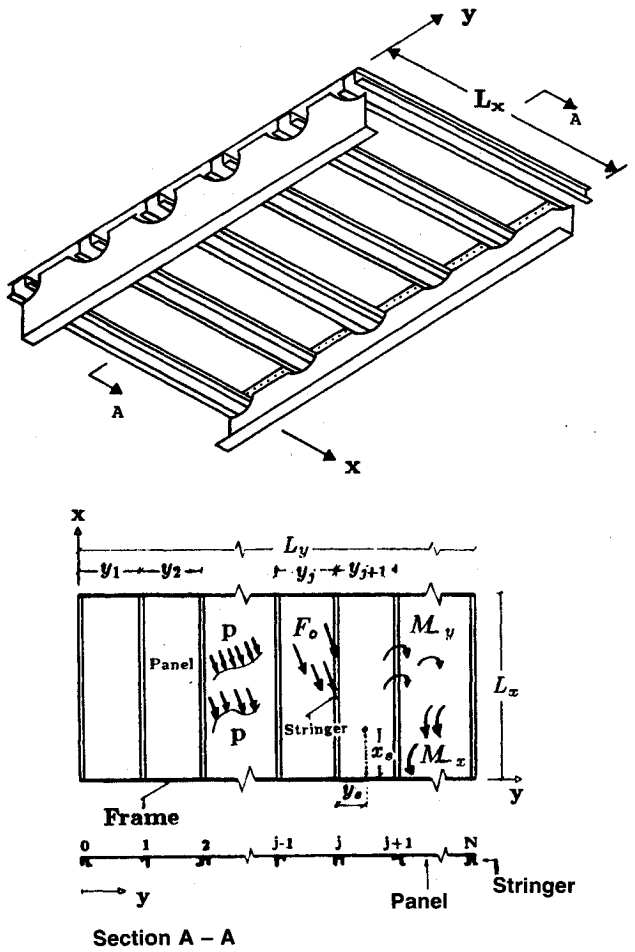

Fig. 1 Stiffened multispanned panel array.

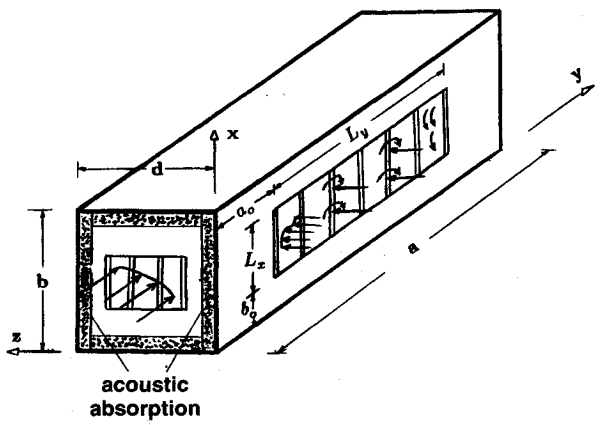

Fig. 2 Geometry of an acoustic enclosure and a stiffened structure.

are characterized by linear coefficients of hygroscopic expansion.[15-17] The constitutive equation for the kth lamina is given as[15]

$$(\bar{\sigma}_i)_k = (\bar{Q}_{ij})_k(\bar{\epsilon}_j - \bar{\alpha}_j\Delta T - \bar{\beta}_j\Delta M) \qquad (i,j = 1,2,6) \quad (1)$$

where summation exists on the repeated index j, and $[\bar{Q}]_k$ is the reduced stress stiffness matrix for the kth layer,[11,15] $\bar{\alpha}_i$ are the coefficients of thermal expansion, $\bar{\beta}_i$ are the coefficients of hygroscopic expansion, ΔT is the change in temperature distribution, and ΔM is the change in moisture concentration. The temperature and moisture concentration are assumed to be functions of the space variables and time t.

We note that Eq. (1) is given with respect to a nonprincipal coordinate system $(\bar{1},\bar{2},\bar{3})$ or (x,y,z) in the plane of the lamina. Also, $\bar{\alpha}_x = \bar{\alpha}_1$, $\bar{\alpha}_y = \bar{\alpha}_2$, $\bar{\alpha}_{xy} = \bar{\alpha}_6$, and the same for the $\bar{\beta}_i$. The following transformation could be used to relate the coefficients to the principal coordinate system (1,2,3).

$$\bar{\alpha}_x = \alpha_1 m^2 + \alpha_2 n^2 \qquad \bar{\beta}_x = \beta_1 m^2 + \beta_2 n^2$$

$$\bar{\alpha}_y = \alpha_2 m^2 + \alpha_1 n^2 \qquad \bar{\beta}_y = \beta_2 m^2 + \beta_1 n^2$$

$$\bar{\alpha}_{xy} = (\alpha_1 - \alpha_2)mn \qquad \bar{\beta}_{xy} = (\beta_1 - \beta_2)mn \qquad (2)$$

where $m = \cos\theta$, $n = \sin\theta$, and θ is the angle of fiber orientation.

Now, if equivalent force resultants are defined, it is possible to separate the force resultants from the plate response.[15] The equivalent thermal force resultant for the whole laminate of thickness h (see Fig. 3), which consists of N laminae is

$$N_i^T = \sum_{k=1}^{N} \int_{z_{k-1}}^{z_k} (\bar{Q}_{ij})_k \bar{\alpha}_j \Delta T \, dz \qquad (i,j = 1,2,6) \quad (3)$$

in which $N_1 = N_x$, $N_2 = N_y$, and $N_6 = N_{xy}$, and summation exists on the repeated index j. Similarly, the equivalent hygroscopic force resultant is

$$N_i^M = \sum_{k=1}^{N} \int_{z_{k-1}}^{z_k} (\bar{Q}_{ij})_k \bar{\beta}_j \Delta M \, dz \quad (4)$$

In order to characterize the flexural response of the laminate, it is necessary to define the moment resultants.[12] The effective thermal moment is

$$M_i^T = \sum_{k=1}^{N} \int_{z_{k-1}}^{z_k} (\bar{Q}_{ij})_k \bar{\alpha}_j \Delta T z \, dz \quad (5)$$

and the effective hygroscopic moment is

$$M_i^M = \sum_{k=1}^{N} \int_{z_{k-1}}^{z_k} (\bar{Q}_{ij})_k \bar{\beta}_j \Delta M z \, dz \quad (6)$$

The thermal and hygroscopic nature of the anisotropic lamina can be approximated by the classical diffusion equation.[15] For simplicity, the temperature and moisture concentrations are assumed to be functions of a single-space variable z and time t. The classical diffusion equation,[18] which governs the absorption and desportion of moisture is given by Eq. (7). The same equation is also valid for temperature changes.[15]

$$D\Delta M_{,zz} - \Delta M_{,t} = 0 \quad (7)$$

where D is the diffusion constant of the material, and commas denote partial differentiation with respect to the subscribed variables. If the kth (for example) lamina is assumed to be

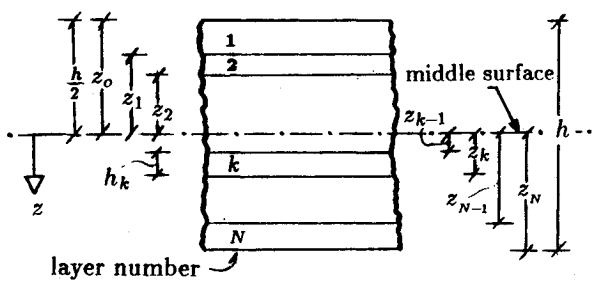

Fig. 3 Geometry of an n-layered laminate.

initially moisture free, while its surfaces $z = \pm h_k/2$ are exposed to moisture concentration ΔM_0, the moisture concentration at position z and time t is[15]

$$\Delta M(z,t) = \Delta M_0 \left\{ 1 - \sum_{n=0}^{\infty} m_n \cos g_n z \right\} \tag{8}$$

where

$$g_n = (2n+1)\pi/h_k \tag{9}$$

and

$$m_n = \frac{(-4)^n}{\pi(2n+1)} \exp[-g_n^2 Dt] \tag{10}$$

Similar solution exists for desportion and single-surface absorption. The same analysis is valid for the temperature concentration function. For the special case when $t \to \infty$, it is $\Delta M = \Delta M_0$ and $\Delta T = \Delta T_0$. Thus, when moisture and temperature have operated for a long time, ΔM and ΔT are not functions of time.

Response of a Stiffened Panel

The noise transmitted into the enclosure shown in Fig. 2 is a function of the sidewall response $w(x,y,t)$. Thus, the response characteristics of a multilayered, composite-stiffened panel has to be determined first. A detailed response analysis has been presented in Refs. 5, 6, and 10. In what follows, a brief description on the calculation of vibration response of a stiffened composite sidewall including the temperature and moisture conentration functions is given.

Consider a flat stiffened panel located on the sidewall at $z=0$, $b_0 \le x \le b_0 + L_x$, $a_0 \le y \le a_0 + L_y$ is simply supported at the edges normal to the stiffeners as shown in Fig. 1. Using classical thin-plate theory, the equation of motion governing the bending vibrations of a symmetrically layered composite panel located between any two arbitrary stiffeners is[10,11,13]

$$D_{11}w_{,xxxx} + 4D_{16}w_{,xxxy} + 2(D_{12}+2D_{66})w_{,xxyy} + 4D_{26}w_{,xyyy} + D_{22}w_{,yyyy} + c\dot{w} + (1+0.01\Delta M_0)\rho h\ddot{w} = p^{\text{rec}} - p^M - p^T + N_x w_{,xx} + N_y w_{,yy} + 2N_{xy}w_{,xy} \tag{11}$$

where $w(x,y,t)$ is the normal deflection, c is the viscous damping coefficient, ρ is the panel mass density, and h is the plate thickness. The factor $(1+0.01\Delta M_0)$ in front of the mass of the plate accounts for the absorbed moisture. The D_{ij} terms are the anisotropic plate rigidity values that relate the internal bending and twisting moments of the plate to the curvatures and twists they induce. We note that D_{ij} terms are functions of time. Also,

$$p^{\text{rec}} = p^r(x,y,t) + p^e(x,y,0,t) + F_0(t)\delta(x-x_0)\delta(y-y_0) + M_y(t)\delta(x-x_0)\delta_{,y}(y-y_0) + M_x(t)\delta_{,x}(x-x_0)\delta(y-y_0) \tag{12}$$

where p^r is the external random pressure, and $p^e(x,y,0,t)$ is the acoustic radiation pressure at $z=0$. When the cavity is sufficiently deep and the plate is sufficiently stiff, it can be taken that $p^e = 0$.[19,20] In Eq. (12), δ is the Dirac delta function, and a prime denotes a derivative. $F_0(t)$ is the random point load, and $M_x(t)$, $M_y(t)$ are the random point couples acting on a plane parallel to x and y, respectively. Also,

$$p^{T,M} = M_x^{T,M}{}_{,xx} + 2M_{xy}^{T,M}{}_{,xy} + M_y^{T,M}{}_{,yy} \tag{13}$$

where M_i^T and M_i^M are given in Eqs. (5) and (6). When moisture and temperature concentration distributions are not functions of x and y, then, it is seen that $p^T = 0 = p^M$. Also in Eq. (11), it is

$$N_i = A_{ij}d_j - N_i^T - N_i^M \qquad (i,j = 1,2,6) \tag{14}$$

in which there is summation on the repeated index j and $d_1 = u_{,x}$, $d_2 = v_{,y}$, $d_6 = u_{,y} + v_{,x}$, with u,v being the in-plane displacements in the x,y direction, respectively. N_i^T and N_i^M are given in Eqs. (3) and (4). The extensional stiffness matrix $[A]$ is given as[12]

$$A_{ij} = \sum_{k=1}^{N} (\bar{Q}_{ij})_k (z_k - z_{k-1}) \tag{15}$$

where z_k is the z-direction distance from the middle surface to the bottom of the kth layer (see Fig. 3).

If the plate is hybrid (differing materials across the thickness) composite, then the total mass density can be calculated from[10,12]

$$\rho = \frac{1}{h} \sum_{k=1}^{N} \rho_k (z_k - z_{k-1}) \tag{16}$$

The flexural rigidities are given as[11,12]

$$D_{ij} = \frac{1}{3} \sum_{k=1}^{n} (\bar{Q}_{ij})_k (z_k^3 - z_{k-1}^3) \tag{17}$$

The theory for calculating the flexural rigidities for tape panels is well established and documented.[11,12] For an orthotropic plate $D_{16} = D_{26} = 0$. Many composite panels, however, are governed by anisotropic behavior where D_{16} and D_{26} are nonzero. A ply that has its fibers parallel to one of the panel boundaries will behave orthotropically. However, for all other fiber orientation angles θ, the ply will behave anisotropically. For the case of many layered symmetric angly-ply laminates, D_{16} and D_{26} are quite small when compared to the other rigidity values D_{ij}, so that orthotropic analysis may be used.[12] Similarly, for an orthotropic plate $\bar{\alpha}_{xy} = \bar{\beta}_{xy} = 0$, and $N_{xy}^T = N_{xy}^M = 0$. For a general anisotropic plate, this is no longer true. However, for the case of many laminates, the contribution of N_{xy}^T and N_{xy}^M in the normal deflection is quite small and can be neglected.[11] The following analysis is based on the previous assumptions.

The solution for the panel deflection w can be written as

$$w(x,y,t) = \sum_{n=1}^{\infty} q_n(y,t) X_n(x) \tag{18}$$

where X_n are the normal modes corresponding to the x direction, and q_n are the generalized coordinates. Since the panel is simply supported at the edges normal to the stiffeners, the normal modes are $X_n = \sin(n\pi x/L_x)$. For different boundary conditions at the edges, different normal modes should be used. Neglecting the in-plane displacements $u = v = 0$ in Eq. (14) and taking $p^M = p^T = 0$ (distributions not functions of x and y), Eq. (11) results in a simpler form. Accepting that all the loads have operated for a long period of time; using all the above mentioned assumptions (i.e., $D_{16} = D_{26} = N_{xy}^T = N_{xy}^M = p^e = 0$); taking Fourier transformation of Eqs. (3) and (4), (11–14), and (18); and following the Galerkin procedure, Eq. (11) reduces to

$$\frac{d^4\bar{q}_n}{dy^4} - 2e_1 \frac{d^2\bar{q}_n}{dy^2} + e_2\bar{q}_n = Q_n \tag{19}$$

where

$$e_1 = \left(\frac{n\pi}{L_x}\right)^2 \frac{D_3}{D_{22}} - \frac{A_{y\alpha\beta}}{2D_{22}} \tag{20}$$

$$e_2 = \left(\frac{n\pi}{L_x}\right)^4 \frac{D_{11}}{D_{22}} + \frac{ic\omega}{D_{22}} - \frac{\rho h\omega^2}{D_{22}} - \left(\frac{n\pi}{L_x}\right)^2 \frac{A_{y\alpha\beta}}{2D_{22}} \tag{21}$$

$$D_3 = D_{12} + 2D_{66} \tag{22}$$

$$\underline{i} = \sqrt{-1} \tag{23}$$

$$A_{x\alpha\beta} = \sum_{k=1}^{N} \left[(\bar{Q}_{1j})_k \bar{\alpha}_j \Delta T_0 + (\bar{Q}_{1j})_k \bar{\beta}_j \Delta M_0\right](z_k - z_{k-1}) \tag{24}$$

$$A_{y\alpha\beta} = \sum_{k=1}^{N} \left[(\bar{Q}_{2j})_k \bar{\alpha}_j \Delta T_0 + (\bar{Q}_{2j})_k \bar{\beta}_j \Delta M_0\right](z_k - z_{k-1}) \tag{25}$$

with summation on the repeated index j and $j = 1,2,6$. Also,

$$Q_n(y,\omega) = \frac{2}{D_{22}L_x}\left[\int_0^{L_x} \bar{p}^r(x,y,\omega)X_n(x)\,dx + \bar{F}_0(\omega)X_n(x_0)\delta(y-y_0) + \bar{M}_y(\omega)X_n(x_0)\delta_{,y}(y-y_0) + \bar{M}_x(\omega)X_{n,x}(x_0)\delta(y-y_0)\right] \tag{26}$$

The roots of the characteristic equation resulting from Eq. (19) are $\pm\sigma_{1n}$, $\pm\underline{i}\sigma_{2n}$, where

$$\sigma_{1n,2n} = \left(\sqrt{e_1^2 - e_2} \pm e_1\right)^{1/2} \tag{27}$$

The solution to Eq. (5) can be written as a superposition of homogeneous and particular solutions[9,10]

$$\bar{q}_n(y,\omega) = \sum_{i=0}^{3} C_{in} f_{in}(y) + \int_0^y f_{3n}(y-\xi)Q_n(\xi,\omega)\,d\xi \tag{28}$$

where C_{in} are arbitray constants to be determined from the boundary conditions, and functions $f_{in}(y)$ are given in Refs. 9 and 10. Differentiating Eq. (19) and introducing the relationships between various derivatives of $\bar{q}_n(y,\omega)$ in terms of slope, bending moment, and shear, the response of an orthotropic panel can be written in a convenient state vector form[4-9]

$$\{Z_n\} = \{\delta_n, \theta_n, M_n, V_n\}^T \tag{29}$$

where δ_n, θ_n, M_n, and V_n are modal components of deflection, slope, moment, and shear, respectively: superscript T denotes the transpose of the matrix. Then, the response state vector at station j on the panel is

$$\{Z_n\}_j^l = [F]_j \{Z_n\}_{j-1}^r + \int_0^{y_j} \left[F(y_j - \xi)\right]\left\{K_n(\xi)\right\} d\xi \tag{30}$$

where the superscripts l and r indicate either the left or right side of station j, respectively, and $\{K_n(\xi)\}$ is the matrix of generalized random forces

$$\left\{K_n(\xi)\right\} = \left\{0,0,0,D_{22}Q_n(\xi,\omega)\right\}^T \tag{31}$$

Also, $[F]$ is the field transfer matrix that transfers the state vector across the composite panel

$$[F]_j = [B]_j [R]_j [B]_j^{-1} \tag{32}$$

with matrices $[R]$ and $[B]$ having the same form as that given in Ref. 10.

To transfer a state vector across the stiffeners, point transfer matrices need to be developed. In addition to bending and twisting, thermal and hygrothermal effects may also be induced. Modified point transfer matrices have been developed to account for these effects.[7] The transfer across a stiffening element at station j is

$$\{Z_n\}_j^r = [G]_j \{Z_n\}_j^l \tag{33}$$

where $[G]$ is the point transfer matrix. Deflections and slopes remain unchanged but moment and shear components of the state vector are affected by the stiffeners.[9,10] We note that for cases in which the stiffener's material is orthotropic and the fiber orientation does not coincide with the stringer's natural axis, a transformation should be used to determine the stiffener's modulus of elasticity.[10] Now the state vector for a multibay panel shown in Fig. 1 can be expressed at any orbitrary location s, where $s = y_s + \Sigma_{m=1}^{j} y_m$, as[9]

$$\{Z_n\}_s^l = {}_s^l[T]_0^l \{Z_n\}_0^l + {}_s^l\{E_n\}_0^l \tag{34}$$

where matrix ${}_s^l[T]_0^l$ transfers the state vector from station 0 to station s and is given in Refs. 9 and 10. Transfer matrix ${}_s^l\{E_n\}_0^l$ represents the effect of distributed and concentrated loads.[6,9]

The solution for the state vector $\{Z_n\}_0^l$ in Eq. (34) can be obtained by applying boundary conditions at $y = 0$ and $y = L$. In this approach, boundaries corresponding to simple, fixed, free, or elastic supports can be considered. Then, after the solution for the state vector $\{Z_n\}_0^l$ is known, using Eq. (34) the response state vector at location s, $\{Z_n\}_s^l$ can be expressed as

$$\{Z_n\}_s^l = -\begin{bmatrix} t_{1k} & t_{1l} \\ t_{2k} & t_{2l} \\ t_{3k} & t_{3l} \\ t_{4k} & t_{4l} \end{bmatrix}_s^l \left({}_N^r\begin{bmatrix} t_{ek} & t_{el} \\ t_{fk} & t_{fl} \end{bmatrix}_0^l \right)^{-1} {}_N^r\begin{Bmatrix} E_e \\ E_f \end{Bmatrix}_0^l + \begin{Bmatrix} E_1 \\ E_2 \\ E_3 \\ E_4 \end{Bmatrix}_s^l \tag{35}$$

where the t_{ij} element is the (i,j) element of matrix $[T]$; E_i is the ith element of matrix $\{E\}$; and (k,l) denote the matrix elements corresponding to boundary conditions at the extreme left end (station 0):

$$(k,l) = \begin{cases} (2,4) & \text{simple} \\ (3,4) & \text{fixed} \\ (1,2) & \text{free} \end{cases} \tag{36}$$

Similarly, (e,f) denote matrix elements according to boundary conditions at the extreme right end (station N):

$$(e,f) = \begin{cases} (1,3) & \text{simple} \\ (1,2) & \text{fixed} \\ (3,4) & \text{free} \end{cases} \tag{37}$$

Finally, the response state vector in terms of displacement, slope moment, and shear can be obtained at any arbitrary location on the stiffened panel from

$$\left\{W(x,\omega)\right\}_s^l = \sum_{n=1}^{\infty} \{Z_n\}_s^l X_n(x) \tag{38}$$

The displacement component $\bar{w}_s(x,\omega)$ (the first element of vector $\{W(x,\omega)\}$) from Eq. (38) will be used to obtain a solution for the acoustic pressure inside the enclosure.

Utilizing the theory of random processes, the response spectral densities corresponding to the four elements in the state vector can be obtained from Eq. (35). For example, the deflection response spectral density at location s can be calculated from

$$S^s(x,\omega) = \sum_{n=1}^{\infty}\sum_{m=1}^{\infty} S^s_{\delta_n\delta_m}(\omega)X_n(x)X_m(x) \tag{39}$$

where $S^s_{\delta_n\delta_m}(\omega)$ is the cross spectral density of the amplitude δ_n^s determined from Eq. (35).

Sound Transmission into Enclosures

Consider a rectangular acoustic space occupying a volume $V = abd$ as shown in Fig. 2, surrounded by a wall surface S, of which a portion S_F is flexible; while the remainder S_R is rigid. The interior surface of the enclosure is assumed to be covered with absorptive materials for which the impedance characteristics are specified. Noise is generated in the acoustic enclosure through the vibration of the flexible portions of the composite sidewall, the partitions or the sound sources located in the interior. Assuming the fluid within the cavity is at rest prior to the flexible wall motion, the perturbation pressure p within the enclosure satisfies the linearized acoustic wave equation[5,8,9,21]

$$\nabla^2 p(\underline{x},t) + \zeta \dot{p}(\underline{x},t) - \frac{\ddot{p}(\underline{x},t)}{c_0^2} + \rho_f \dot{s}\delta(\underline{x}-\underline{x}_0) = 0 \qquad (40)$$

where a dot denotes derivative with respect to time, ∇^2 is the Laplacian operator $\nabla^2 = \partial^2/\partial x^2 + \partial^2/\partial y^2 + \partial^2/\partial z^2$; δ is the Dirac delta function, which locates the point source; $\underline{x}_0 = x_0, y_0, z_0$, $\underline{x} = x, y, z$, and $\zeta, c_0, \rho_f, \dot{s}(t)$ are the acoustic damping coefficient, speed of sound, and fluid density and flow rate, respectively.

At boundaries where a sound absorptive material is attached to flexible vibrating surface (as shown in Fig. 2), the interface displacement w_t can be written as

$$w_t = w_F + w_A \qquad (41)$$

where $w_F \equiv w$ is the flexible wall displacement, and w_A is the deformation of the absorptive material.

Utilizing a bulk reaction model[22] and satisfying compatibility of the normal fluid velocity components, the boundary conditions to be used to solve Eq. (40) are

$$\frac{\partial p}{\partial n} = -\rho_f \ddot{w}_F - \frac{\rho_f(\dot{p} + B(\omega)\nabla_s^2 \dot{p})}{Z_A(\omega)} \qquad \text{on } S_F \qquad (42)$$

$$\frac{\partial p}{\partial n} = -\frac{\rho_f(\dot{p} + B(\omega)\nabla_s^2 \dot{p})}{Z_A(\omega)} \qquad \text{on } S_R \qquad (43)$$

where n is the outward normal to the boundary; Z_A, B, ∇_s^2 are, respectively, the absorbent wall impedance, bulk reactance, and the Laplacian at the interior surface boundary.

Consider the noise problem shown in Fig. 2 where sound is generated only by a vibrating composite stiffened panel located at $z = 0$. The interior surfaces at $z = 0$ and $z = d$ are assumed to be absorbent, whereas the remaining interior surfaces are assumed to be acoustically hard. The effect of acoustic absorption from those surfaces is included in approximation through the acoustic damping coefficient ζ.[23] Assuming that the random loading causing the vibrations of the composite stiffened panel has operated for a sufficiently long time so that the effects of the initial conditions have died out, a solution can be developed in frequency domain.

The acoustic pressure can be expressed in terms of orthogonal modes[8,9] corresponding to acoustically hard walls at $x = 0, b$ and $y = 0, a$ as follows

$$p(x,y,z,t) = \sum_{i=0}^{\infty}\sum_{j=0}^{\infty} P_{ij}(z,t)\, Y_{ij0}(x,y) \qquad (44)$$

in which P_{ij} are the acoustic modal coefficients, Y_{ijk} are the acoustic hard wall modes[21]

$$Y_{ijk}(x,y,z) = \cos\left(\frac{i\pi x}{b}\right)\cos\left(\frac{j\pi y}{a}\right)\cos\left(\frac{k\pi z}{d}\right) \qquad (45)$$

and a bar indicates a Fourier transform of the quantity. The modal acoustic frequencies corresponding to these modes are

$$\omega_{ijk} = c_0\left[\left(\frac{i\pi}{b}\right)^2 + \left(\frac{j\pi}{a}\right)^2 + \left(\frac{i\pi}{d}\right)^2\right]^{1/2} \qquad (46)$$

where a, b, d are dimensions of the rectangular enclosure.

Using Eq. (42) for $z = 0$, Eq. (43) for $z = d$, taking the Fourier transformation of Eqs. (40), (42), and (43), setting $\dot{s} = 0$; and writing the solution in terms of acoustic modes [Eq. (44)], it can be shown that

$$\bar{p}(x,y,z,\omega) = \sum_{i=0}^{\infty}\sum_{j=0}^{\infty} \frac{G_{ij0}}{(\lambda_{ij0})(k_{ij0}^2 + 2k_{ij0}\cot\lambda_{ij0}d - 1)(\sin\lambda_{ij0}d)} \times V_{ij}(z,\omega) \times Y_{ij0} \qquad (47)$$

where

$$\lambda_{ijk}^2 = \frac{\omega^2 - \omega_{ijk}^2}{c_0^2} + \underline{i}\omega\zeta \qquad (48)$$

$$k_{ijk}(\omega) = \left(\frac{\underline{i}\omega\rho_f}{Z_A}\right)\frac{b_{ijk}}{\lambda_{ijk}} \qquad (49)$$

$$b_{ijk} = 1 - B\frac{\omega_{ijk}^2}{c_0^2} \qquad (50)$$

$$V_{ij}(z,\omega) = \cos[\lambda_{ij0}(d-z)] + k_{ij0}\sin[\lambda_{ij0}(d-z)] \qquad (51)$$

$$G_{ij0}(\omega) = \frac{1}{ba\epsilon_{ij}}\iint_{S_F} \rho_f\omega^2 \bar{w}(x,y,\omega)\, Y_{ij0}(x,y)\, dx\, dy \qquad (52)$$

$$\epsilon_{ij} = \begin{cases} 1 & (i=0,\ j=0) \\ 1/2 & (i\neq 0 \text{ or } j\neq 0) \\ 1/4 & (i\neq 0,\ j\neq 0) \end{cases} \qquad (53)$$

The spectral density of the interior acoustic pressure $S_{\bar{p}}$ can be obtained by taking the mathematical expectation of Eq. (47) and following the procedures given in Ref. 9. Then,

$$S_{\bar{p}}(x,y,z,\omega) = \sum_{i=0}^{\infty}\sum_{j=0}^{\infty}\sum_{r=0}^{\infty}\sum_{q=0}^{\infty} S_{ijrq}(\omega)\, V_{ij}(z,\omega) \times V_{rq}(z,\omega)\, Y_{ij0}(x,y)\, Y_{rq0}(x,y) \qquad (54)$$

where

$$S_{ijrq} = H_{ij}(\omega)\, I_{ijrq}\, H_{rq}^*(\omega) \qquad (55)$$

in which

$$H_{ij}(\omega) = \frac{\rho_f\omega^2}{(ba\epsilon_{ij}\lambda_{ij0})(k_{ij0}^2 + 2k_{ij0}\cot\lambda_{ij0}d - 1)(\sin\lambda_{ij0}d)} \qquad (56)$$

$$I_{ijrq} = \int_{a_o}^{a_o+L_x}\int_{a_o}^{a_o+L_x}\int_{b_o}^{b_o+L_y}\int_{b_o}^{b_o+L_y} S_{\bar{w}}(x_1,x_2,y_1,y_2,\omega) \times Y_{ij0}\, Y_{rq0}\, dx_1\, dx_2\, dy_1\, dy_2 \qquad (57)$$

where an asterisk indicates a conjugate, and $S_{\bar{w}}(x_1,x_2,y_1,y_2,\omega)$ is the cross-spectral density of the stiffened panel response. We note that, for $x_1 = x_2 = x$ and $y_1 = y_2 = s$, it is $S_{\bar{w}} = S^s$ given in Eq. (39). Then, the sound pressure levels inside the enclosure can be calculated from

$$\mathrm{SPL}(x,y,z,\omega) = 10\log\left\{S_{\bar{p}}(x,y,z,\omega)\frac{\Delta\omega}{p_0^2}\right\} \qquad (58)$$

where $\Delta\omega$ is the frequency bandwidth, and p_0 is reference pressure ($p_0 = 2.9\cdot 10^{-9}$ psi, $p_0 = 20\mu\mathrm{N/m^2}$).

Noise generated in the interior by other vibrating surfaces such as the end plates or partitions can be calculated in a similar fashion. Consider, for example, the enclosure shown in Fig. 2 having flexible vibrating end plates at $y = 0, a$, or more generally, two elastic partitions perpendicular to the y axis located at $y = y_a$ and $y = y_b$ subdividing the rectangular enclo-

sure into three subvolumes. Now Eq. (42) has to be used for $y=y_a$ and $y=y_b$. Also w_1 and w_2 are the normal displacements of vibrating partitions and $w_r=0$, $(r=1,2)$ outside the flexible region of each partition panel. The interior acoustic pressure is now written in terms of orthogonal acoustic modes corresponding to acoustically hard walls at $x=0,b$ and $z=0,d$, i.e.,

$$\bar{p}(x,y,z,\omega)=\sum_{i=0}^{\infty}\sum_{k=0}^{\infty}P_{ik}(y,\omega)\,Y_{i0k}(x,z) \tag{59}$$

Assuming identical interior absorption characteristics of the two interior walls at $y=y_a$ and $y=y_b$, the solution for the interior acoustic pressure is

$$\begin{aligned}\bar{p}(x,y,z,\omega)=&\sum_{i=0}^{\infty}\sum_{k=0}^{\infty}\\&\times\frac{Y_{i0k}}{(\lambda_{i0k})(k_{i0k}^2+2k_{i0k}\cot\lambda_{i0k}a_1-1)(\sin\lambda_{i0k}a_1)}\\&\times\Big\{\Big[\cos\big[\lambda_{i0k}(y_b-y)\big]+k_{i0k}\sin\big[\lambda_{i0k}(y_b-y)\big]\Big]G_{1_{i0k}}\\&+\Big[\cos\big[\lambda_{i0k}(y-y_a)\big]+k_{i0k}\sin\big[\lambda_{ij0}(y-y_a)\big]\Big]G_{2_{i0k}}\Big\}\end{aligned} \tag{60}$$

where $a_1=y_b-y_a$, $y_a\le y\le y_b$ and

$$G_{r_{i0k}}(\omega)=\frac{1}{bd\epsilon_{ik}}\iint_{S_{F_r}}\rho_f\omega^2\bar{w}_r(x,y,\omega)\,Y_{i0k}(x,y)\,dx\,dz;\qquad r=1,2 \tag{61}$$

in which $\lambda_{i0k}, k_{i0k}, \epsilon_{ik}$ are previously defined in Eqs. (48), (49), and (53), respectively. The spectral density can be obtained similarly as before.

Noise generated in the interior by other vibrating surfaces can be estimated by the procedure presented above. Then, the total acoustic pressure inside the enclosure can be obtained from[9]

$$p=p_1+p_2+\cdots+p_m \tag{62}$$

where $p_1,p_2,\cdots,p_m$ are the acoustic pressure contributions from the vibrating walls that surround the enclosure. If those pressure contributions are assumed to be independent, the cross-spectral densities corresponding to the various pressure components can be set equal to zero, thereby simplifying the calculation procedure.

We note that having a structural solution in closed form enables us to compute the acoustic pressure without any numerical integration. Evaluation of integrals is calculated in closed form.[9]

Numerical Results

In order to determine the importance of hygrothermal loads, numerical results were obtained for simplified versions of the stiffened structure shown in Figs. 1 and 2. The stiffened panel is composed of three equal bays. Two stiffeners are located at the boundaries, and others are placed at a distance $y_1=y_2=8.2$ in. (see Fig. 4). The physical parameters for the panel and the stiffeners are typical of those of a transport jet aircraft.[4,9] The flexible panel has $L_x=20$ in. and $L_y=24.6$ in. The physical parameters for the stiffeners are cross-sectional area $A=0.2302$ in.^{2}, warping constant $C_{ws}=0.01649$ in.^{6}, torsion constant $C=2.263\times10^{-4}$ in.^{4}, moments of inertia $I_\eta=0.122$ in.^{4}, $I_{\eta\zeta}=0.0$, and $I_\zeta=0.083$ in.^{4}. The material for the isotropic panel is aluminum and for the composite panel is graphite-epoxy. The composite panel consists of symmetrically laminated plies with the stacking sequence, $[0/45/-45/90]_{4s}$. The ply properties for the graphite-epoxy composite are $E_{11}=21\times10^6$ psi, $E_{22}=1.7\times10^6$ psi, $G_{12}=0.65\times10^6$ psi, $\alpha_1=2.1\times10^{-6}/°\text{F}$, $\alpha_2=16\times10^{-6}/°\text{F}$, all in room temperature. At $\Delta T_0=20°\text{F}$ the temperature dependent properties are $E_{11}=20.83\times10^6$ psi, $E_{22}=1.64\times10^6$ psi, $G_{12}=0.6265\times10^6$ psi, $\alpha_1=2.5\times10^{-6}/°\text{F}$, $\alpha_2=16.415\times10^{-6}/°\text{F}$. A linear variation was assumed between 0 and $\Delta T_0=20°\text{F}$. Additional lamina properties were $\nu_{12}=0.31$, $h_k=0.0055$ in., $\rho_k=1.373\times10^{-4}$ lb·s^2/in.^{4}, $\beta_1=0$, and $\beta_2=4.75\times10^{-3}$/wt%. For the aluminum, $E=10.5\times10^6$ psi (room temperature), $E=10.3\times10^3$ psi (at $\Delta T_0=20°\text{F}$), $\nu=0.3$, $\rho=2.617\times10^{-4}$ lb·s^2/in.^{4}, $\alpha_1=\alpha_2=12.8\times10^{-6}/°\text{F}$ (at room temperature), and $\alpha_1=\alpha_2=13\times10^{-6}/°\text{F}$ (at $\Delta T_0=20°\text{F}$). Damping in the skin-stringer structure is introduced by replacing E_{11}, E_{22}, G_{12} by $E_{11}(1+ig_{11})$, $E_{22}(1+ig_{22})$, $G_{12}(1+ig_{12})$, respectively, where g_{11}, g_{22}, g_{12} are the los factors. Numerical results were obtained for $g_{11}=g_{22}=g_{12}=0.02$. The forcing function has the simple form of point forces F_i applied on the stiffeners as shown in Fig. 4. The four point forces are assumed to be characterized by truncated Gaussian white noise spectral densities

$$S_{F_i}(f)=\begin{cases}0.00084\ \text{lb}^2/\text{Hz} & 0\le f\le f_u\\ 0 & \text{otherwise}\end{cases} \tag{63}$$

where f is the frequency in Hz, $i=1,2,3,4$, and f_u is the upper cutoff frequency. These point loads are located at the positions as indicated in Fig. 4.

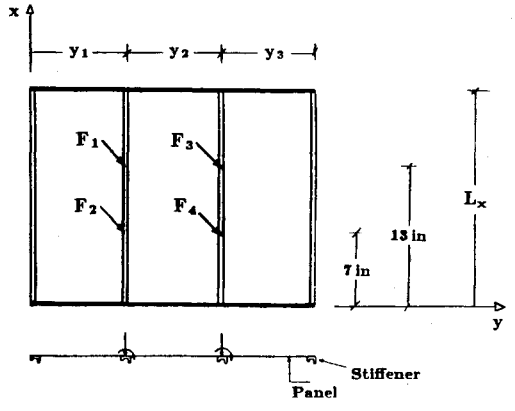

Fig. 4 A three-bay stiffened panel.

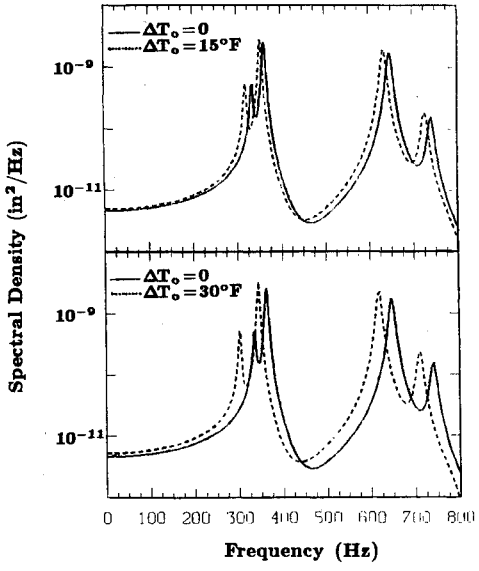

Fig. 5 Deflection response spectral densities to different temperature changes for a composite panel.

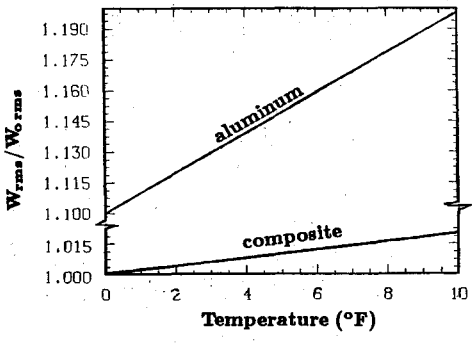

Fig. 6 Root-mean-square displacements for different temperature changes.

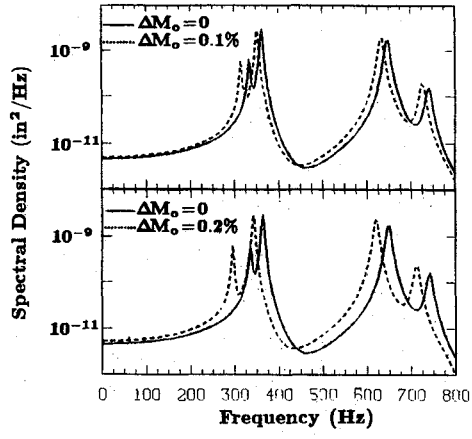

Fig. 7 Deflection response spectral densities for different moisture absorption.

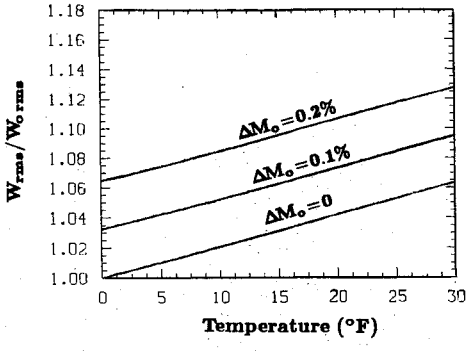

Fig. 8 The rms displacements for different temperature and moisture concentrations.

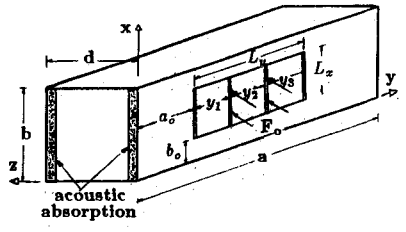

Fig. 9 Geometry of an acoustic enclosure subject to random point loads.

Structural Response

Deflection response spectral densities of the composite panel were obtained for point forces. The results correspond to an upper cutoff frequency $f_u = 800$ Hz. Figure 5 shows the response for a variety of temperature chances ΔT_0. The panel deflection response is calculated at $x = 10$ in., $y = 8.2$ in. The reference point is at the middle of the first stringer. Depending on the value of ΔT_0, significant differences in response values and resonant frequencies are obtained. It can be observed that as the temperature is increased, the resonant frequencies move to the left (lower frequencies) and the total amplitude increases. This is because the stiffness of the material is reduced when heated. The behavior of an equivalent aluminum panel is similar to the composite one. Figure 6 shows the total root-mean-square deflection response W_{rms} as a function of temperature changes. The rms deflection (on the vertical axis) is normalized with respect to the total rms deflection $W_{0\text{rms}}$ corresponding to $\Delta T_0 = 0$. Aluminum is more sensitive to changes in temperature since the coefficients of thermal expansion were taken to be of greater magnitude. A significant amount of response reduction can be achieved by using composite materials.

The effect of moisture concentration was also studied. Figure 7 illustrates the effect of moisture concentration. Moisture is increased from 0 to 0.1 and 0.2%. Behavior is similar to the temperature effects. Stiffness is reduced as moisture increases. Thus, deflection amplitude increases and resonant frequencies move to lower levels. Temperature and moisture effects on the total rms deflection response are presented in Fig. 8. The rms response is again normalized with respect to $W_{0\text{rms}}$, which corresponds to $\Delta T_0 = \Delta M_0 = 0$. Thus, the moisture effects are identically analogous to thermal effects. Hygrothermal loads are very important in predicting plate deflections.

Sound Transmission

For the calculation of noise transmission into the enclosure, a simplified model shown in Fig. 9 has been chosen. The stiffened panel is again composed of three equal bays. Random point external loads are acting at the stiffeners; thermal and hygrothermal loads are acting on the stiffened panels. The walls at $z = 0$ and $z = d$ of the acoustic enclosure are treated with absorptive materials, which are represented by the point impedance model as

$$Z_A(\omega) = Z_R + iZ_I \tag{64}$$

where for acoustic materials, the resistance Z_R and the reactance Z_I are given by[21]

$$Z_R = \rho_f c_0 \left[1 + 0.0571 \left(\frac{2\pi R}{\rho_f \omega} \right)^{0.754} \right] \tag{65}$$

$$Z_I = -\rho_f c_0 \left[0.087 \left(\frac{2\pi R}{\rho_f \omega} \right)^{0.732} \right] \tag{66}$$

in which $\rho_f c_0$ is the characteristic impedance, and R is the flow resistivity of the absorbing materials. The results presented in this paper are obtained for resistivity $R = 4 \times 10^4$ mks rayls/m and for bulk reaction coefficient $B(\omega) = 0$.

The numerical results were obtained for $a = 142$ in., $b = 50$ in., $d = 48$ in., $a_o = 60$ in., $b_o = 15$ in., $y_1 = y_2 = y_3 = 8.2$ in., $L_x = 20$ in., and $L_y = 24.6$ in. Interior noise in the enclosure was calculated at $x = 25$ in., $y = 71$ in., and $z = 24$ in. The acoustic damping coefficient ζ was related to the acoustic modal damping ratios ξ_{ij} by[23]

$$\xi_{ij} = \frac{\zeta c_0^2}{2\omega_{ij0}} \tag{67}$$

where $\zeta c_0^2 = 2\omega_0 \xi_0$, in which ω_0 is the lowest acoustic modal frequency chosen from ω_{001}, ω_{010}, and ω_{100} (i.e., ω_{010} in our case). The damping ratio corresponding to the fundamental acoustic mode $\xi_0 = 0.03$ takes into account the contributions of all the damping effects of the acoustic space. Air density and speed of sound in the enclosure are $\rho_f = 1.147 \times 10^{-7}$ lb$_f \cdot$ s^2/in.^{4} and $c_0 = 13{,}540$ in./s, respectively. All the calculations are

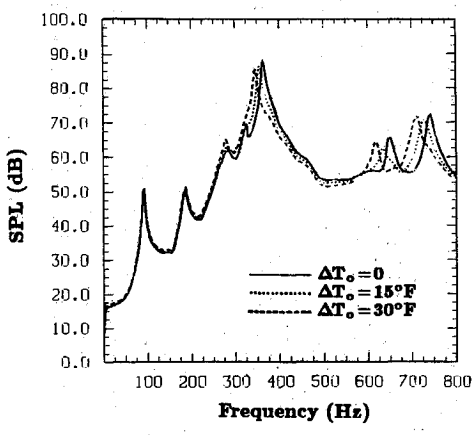

Fig. 10 Sound pressure levels in the interior for different temperature changes.

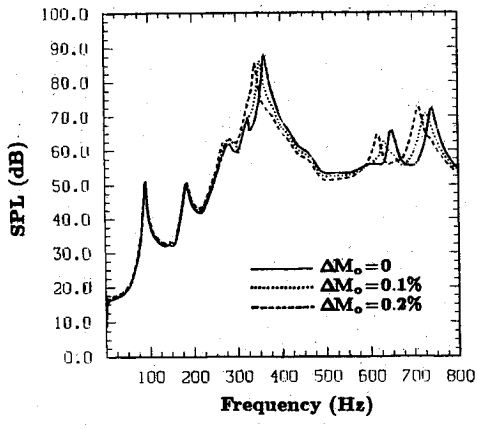

Fig. 11 Sound pressure levels for different moisture concentrations.

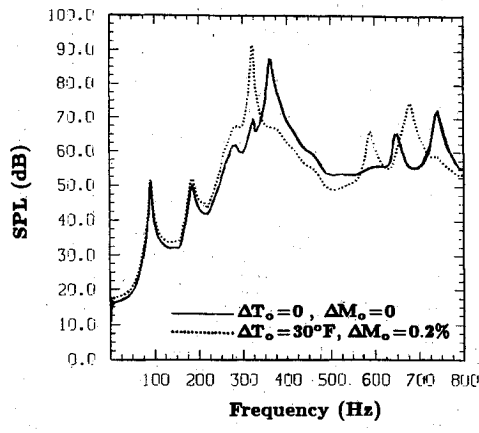

Fig. 12 Sound pressure levels in the interior for different temperature and moisture concentrations.

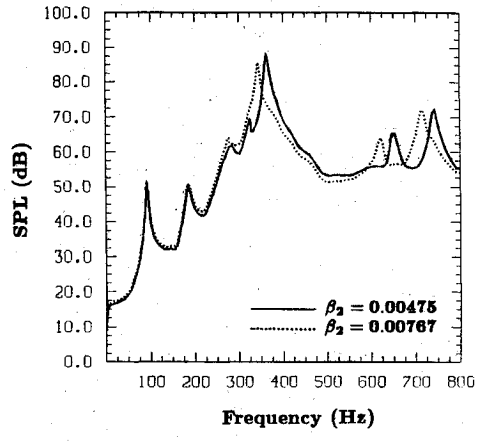

Fig. 13 Sound pressure levels for different coefficients of hygroscopic expansion.

based on a frequency bandwidth $\Delta f = 1$ Hz. The inputs to the stiffened panel are four-point forces acting on the two intermediate stringers (see Fig. 9) for which the spectral densities are given in Eq. (63). The walls are treated with porous materials for which the point impedance is given in Eqs. (64–66).

Sound pressure levels are given in Fig. 10 for an acoustic enclosure subjected to temperature changes 0 to 15 and 30° F. Resonances corresponding to structural modes move to lower frequencies as the stiffness reduces. Resonances corresponding to acoustic modes do not change. Analogous results are obtained for different hygrothermal loads. Figure 11 depicts sound pressure levels in the interior of the acoustic enclosure for different moisture concentrations. Transmitted noise is very sensitive to changes in moisture concentrations and is imperative to be included in transmitted sound predictions. A combined temperature and moisture effect is shown in Fig. 12. The argument that higher temperatures result in higher deflection amplitudes and then to higher overall noise levels might not always be true since overall transmitted noise levels are dominated by the coupling of the composite structural modes and the acoustic modes. When the natural frequency of one of the composite-stiffened panel modes coincides with one acoustic mode, a strong peak appears in the sound pressure levels curve (see Fig. 12). This peak dominates the overall noise. Small changes in temperature may result in significant changes in noise levels.

Results are also very sensitive to accurate specifications of the hygroscopic coefficient of the material. A comparison of the sound pressure levels for different coefficients of hygroscopic expansion, $\beta_2 = 4.75 \times 10^{-3}$/wt% and $\beta_2 = 7.67 \times 10^{-3}$/wt%, is given in Fig. 13. The transmitted noise is always a function of the type of vibrating flexible surface. The interior noise levels may be tailored to meet specific needs by selecting a suitable material.

Conclusions

An analytical method based on transfer matrices has been developed for analyzing the dynamic response, noise generaton, and transmission of a stiffened composite panel including the temperature and moisture effects. The formulation can be applied to a variety of discretely stiffened composite and isotropic structures. In addition, it has been shown that structural response and transmitted noise levels in the interior are sensitive to changes in temperature and moisture concentrations. Moisture effects on panel response and noise transmission are similar to thermal effects. It was found that increasing temperature and/or moisture results in higher response levels. Resonances corresponding to structural modes of the stiffened panel move to lower frequencies as the stiffness reduces. In general, the response levels for a composite-stiffened panel are much lower than those of an equivalent aluminum-stiffened panel. The interior noise is strongly dependent on the thermal and hygrothermal loads. An increase in temperature and/or absorbed moisture on the composite flexible surface tends to move the structural modes to lower frequencies, leaving the acoustic modes unchanged. Overall noise levels are dominated by the coupling of structural and acoustic modes. Transmitted sound and structural response are very sensitive to the dynamic characteristics of the stiffened sidewall. Thus, coefficients of thermal and hygrothermal expansion should be precisely identified.

The results indicate that thermal and moisture effects are very important in predicting deflections and transmitted noise. Therefore, it is imperative that the effects be accounted for in the design of composite airframe structures.

Acknowledgment

C. S. Lyrintzis was supported in part by a grant from the San Diego State University Foundation.

References

[1]Mixson, J. S., and Wilby, J. F., "Airplane Interior Noise: A Status Review," AIAA Paper 87-2659, Oct. 1987.

[2]Bofilios, D. A., and Vaicaitis, R., "Response of Double Wall Composite Shells to Random Point Loads," *Journal of Aircraft,* Vol. 24, No. 4, 1987, pp. 268–273.

[3]Vaicaitis, R., and Bofilios, D. A., "Noise Transmission of Double Wall Composite Shells," AIAA Paper 86-1937, July 1986.

[4]Lin, Y. K., and Donaldson, B. K., "A Brief Survey of Transfer Matrix Techniques with Special Reference to Aircraft Panels," *Journal of Sound and Vibration,* Vol. 10, No. 1, 1969, pp. 103–143.

[5]Lyrintzis, C. S., and Vaicaitis, R., "Structure-borne Noise Generation and Transmission," *Journal of Probabilistic Engineering Mechanics,* Vol. 2, No. 3, 1987, pp. 114–120.

[6]Vaicaitis, R., and Lyrintzis, C. S., "Response of Discretely Stiffened Structures," AIAA Paper 87-0914, April 1987.

[7]Vaicaitis, R., and Choi, S. T., "Response of Stiffened Panels for Applications to Acoustic Fatigue," AIAA Paper 87-2711, Oct. 1987.

[8]Vaicaitis, R., and Slazak, M., "Noise Transmission Through Stiffened Panels," *Journal of Sound and Vibration,* Vol. 70, No. 3, 1980, pp. 413–426.

[9]Lyrintzis, C. S., "Response of Discretely Stiffened Structures and Transmission of Structure-borne Noise," Doctoral Thesis, Department of Civil Engineering and Engineering Mechanics, Columbia Univ., New York, 1987.

[10]Lyrintzis, C. S., and Vaicaitis, R., "Random Response and Noise Transmission of Discretely Stiffened Composite Panels," *Journal of Aircraft,* Vol. 27, No. 2, 1990, pp. 176–184.

[11]Vinson, J. R., and Sierakowski, R. L., *The Behavior of Structures Composed of Composite Materials,* Kluwer, Hingham, MA, 1986.

[12]Jones, R. M., *Mechanics of Composite Materials,* Scripta, Washington, DC, 1975.

[13]Boley, B. B., and Weiner, J. H., *Theory of Thermal Stresses,* Wiley, New York, 1960.

[14]Soovere, J., "The Effect of Acoustic/Thermal Environments on Advanced Composite Fuselage Panels," *Journal of Aircraft,* Vol. 10, No. 4, 1985, pp. 257–263.

[15]Pipes, R. B., Vinson, J. R., and Chou, T. W., "On the Hygrothermal Response of Laminated Composite Systems," *Journal of Composite Materials,* Vol. 10, April 1976, pp. 129–148.

[16]Flaggs, D. L., and Vinson, J. R., "Hygrothermal Effects on the Buckling of Laminated Composite Plates," *Journal of Fibre Science and Technology,* Vol. 11, April 1978, pp. 353–365.

[17]Kim, R. Y., and Whitney, J. M., "Effect of Temperature and Moisture on Pin Bearing Strength of Composite Laminates," *Journal of Composite Materials,* Vol. 10, April 1976, pp. 149–155.

[18]Jost, W., *Diffusion in Solids, Liquids, Gases,* Academic, New York, 1960.

[19]Dowell, E. F., and Voss, H. M., "The Effect of Cavity on Panel Vibrations," *AIAA Journal,* Vol. 1, 1963, pp. 476–477.

[20]McDonald, W. B., Vaicaitis, R., and Myers, M. K., "Noise Transmisson Through Plates into an Enclosure," NASA TP-1173, 1978.

[21]Beranek, L. L., *Noise and Vibration Control,* McGraw-Hill, New York, 1971.

[22]Bliss, D. B., "Study of Bulk Reacting Porous Sound Absorbers and a New Boundary Condition for Thin Porous Layers," *Journal of the Acoustical Society of America,* Vol. 71, No. 3, 1982, pp. 533–545.

[23]Dowell, E. H., Gorman, G. F., and Smith, D. A., "Acoustoelasticity: General Theory, Acoustic Natural Modes and Forced Response to Sinusoidal Excitation, Including Comparisons with Experiment," *Journal of Sound and Vibration,* Vol. 52, June 1977, pp. 519–592.